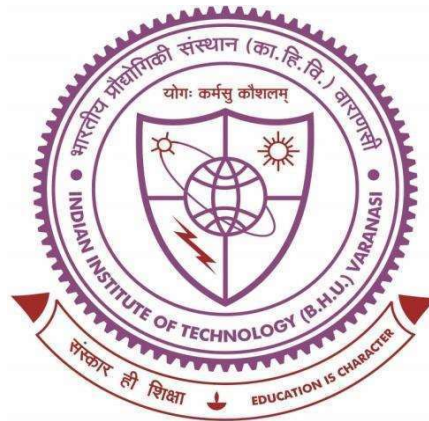


Computational Analysis of alteration of Visual Perception under specific external and internal factors



**Thesis submitted in partial fulfillment
for the Award of Degree**

Doctor of Philosophy

by

Pratik Purohit

**SCHOOL OF BIOMEDICAL ENGINEERING
INDIAN INSTITUTE OF TECHNOLOGY
(BANARAS HINDU UNIVERSITY)
VARANASI – 221005
INDIA**



SCHOOL OF BIOMEDICAL ENGINEERING
INDIAN INSTITUTE OF TECHNOLOGY
B.H.U., Varanasi – 221005
India

CERTIFICATE

It is certified that the work contained in the thesis titled “**Computational Analysis of Alteration of Visual Perception under specific external and internal factors**” by “**Pratik Purohit**” has been carried out under my supervision and this work has not been submitted elsewhere for a degree.

It is further certified that the student has fulfilled all the requirements of Comprehensive Examination, Candidacy and SOTA for the award of Ph.D. Degree.

Prasun Roy

(Prof. Prasun Kumar Roy)
Supervisor

Dr. Shiru Sharma

(Dr. Shiru Sharma)
Co-supervisor

Date: 27/7/23

Place: Varanasi, India.



SCHOOL OF BIOMEDICAL ENGINEERING
INDIAN INSTITUTE OF TECHNOLOGY
B.H.U., Varanasi – 221005
India

DECLARATION BY THE CANDIDATE

I, Pratik Purohit, certify that the work embodied in this Ph.D. thesis is my bonafide work and was carried out by me under the supervision of Prof. Prasun Kumar Roy and Dr. Shiru Sharma from 27th December 2017 to 27th July 2023 at the School of Biomedical Engineering, Indian Institute of Technology (BHU), Varanasi, India. The matter embodied in this thesis has not been submitted for the award of any other degree/diploma.

I declare that I have faithfully acknowledged and given credits to the research workers wherever their work has been cited in my work in this thesis. I further declare that I have not wilfully copied any other's work, paragraphs, text, data, results, etc., reported in journals, books, magazines, reports, dissertations, theses, etc., or available on websites and have not included them in this thesis and have not cited as my work.


Date: 27/07/2023

Place: Varanasi, India


Signature of the Student
(Pratik Purohit)

CERTIFICATE BY THE SUPERVISOR

It is certified that the above statement made by the student is correct to the best of our knowledge.


(Prof. Prasun Kumar Roy)
Supervisor


(Dr. Shiru Sharma)
Co-supervisor


Coordinator 27/07/23

School of Biomedical Engineering
Indian Institute of Technology (BHU)
Varanasi – 221005, India.

समन्वयक/CO-ORDINATOR
जैव चिकित्सा अभियांत्रिकी स्कूल
SCHOOL OF BIOMEDICAL ENGG.
भारतीय प्रौद्योगिकी संस्थान (का.हि.वि.)
INDIAN INSTITUTE OF TECHNOLOGY (B.H.U.)
वाराणसी 221005/VARANASI-221005



SCHOOL OF BIOMEDICAL ENGINEERING
INDIAN INSTITUTE OF TECHNOLOGY
B.H.U., Varanasi – 221005
India

COPYRIGHT TRANSFER CERTIFICATE

Title of the Thesis: Computational analysis of alteration of visual perception
under specific external and internal factors.

Submitted by: Pratik Purohit

Copyright Transfer

The undersigned hereby assigns to the Indian Institute of Technology (IIT), Varanasi, India, all rights under copyright that may exist in and for the above thesis submitted for the award of the Doctor of Philosophy.

Date: 27/07/2023

Place: Varanasi, India.


(Pratik Purohit)

Note: However, the author may reproduce or authorize others to reproduce material extracted verbatim from the thesis or derivative of the thesis for the author's personal use, provided that the source and the Institute's copyright notice are indicated.

ACKNOWLEDGEMENTS

With immense gratitude and deep appreciation, I extend my heartfelt acknowledgment to those who helped me during my Ph.D. program at the Indian Institute of Technology (Banaras Hindu University), Varanasi.

First and foremost, I am indebted to my esteemed supervisor, Prof. Prasun Kumar Roy. His invaluable guidance, unwavering encouragement, and unconditional support have been instrumental in shaping my research journey. His inspiring mentorship has been the cornerstone of my success, and I am truly grateful for his dedication and expertise. Without his exceptional guidance, this work would not have been possible.

I am also honored to express my sincere gratitude to Dr. Shiru Sharma. Her excellent supervision, skilled guidance, constant support, and encouragement have been influential in my academic and personal growth. I am indebted to her sincere concern, care, and nurturing environment. I am forever grateful for her affectionate nature and support.

I would like to extend my heartfelt gratitude to Dr. Prasun Dutta, Dept of Physics, for his invaluable feedback and assistance, which proved crucial in successfully completing my work. I am sincerely thankful for his crucial support and the valuable suggestions he provided throughout the process.

I extend my appreciation to the members of my research progress evaluation committee (RPEC), Prof. Neeraj Sharma, Dr. M. S. Muthu, and Dr. Prasanta Kumar Nayak, for their valuable feedback and evaluation of my work. Their expertise and insights have contributed significantly to the refinement of my research. I would like to express my gratitude to Prof. Sanjeev Kumar Mahto, the Coordinator of the School of Biomedical Engineering, for providing all the necessary facilities and resources to support my research endeavors.

I would like to express our heartfelt gratitude to the National Supercomputing Mission, Government of India, for generously providing access to their high-performance computational facility, the Institutional Supercomputing Facility—Param Shivay, located at the Indian Institute of Technology (BHU), Varanasi.

I am privileged to be a part of the School of Biomedical Engineering, and I thank all faculty members for their support. My heartfelt appreciation goes to Dr. Pradip Paik, Dr. Sanjay Kumar Rai, Dr. Sudip Mukherjee, Dr. Gowri Balachander, Dr. A. R. Jac Fredo, Dr. Deepesh Kumar, and Dr. Brijesh Kumar. Their expertise and advice have been invaluable in overcoming the challenges I faced during my doctoral studies.

I am deeply grateful to my lab mates, Bindu Kumari, Anindita Bhattacharjee, Brijesh Baghel, Mahatim Singh, Sumit Swargiary, Kuldeep Kaiwart, Sourav Chowdhury, Yashasvi, Fahad, Naveen, and Dakpin for stimulating discussions and the vibrant atmosphere in the lab. I would also like to thank my batch-mates, Sumit Kumar, Nillmani, Pankaj Jain, Prem Shankar Gupta, and Kirti Wasnik, for their help whenever I needed.

I extend my gratitude to the supporting staff of the School for their kind assistance whenever required. I am thankful to Mr. Bhuwaneshwari Sharan, Dr. Anuj Srivastava, Mr. Avinash Kumar Srivastava, Mr. Divyanshu Singh, Mr. Vipin Kumar Verma, Mr. Ajay Kumar, Mr. Bharat Kumar Vishwakarma, Mr. Kishori Lal, and Mr. Parmatma Nand Singh, for their support and cooperation throughout my doctoral program.

I would like to take this moment to express my deepest appreciation and gratitude to the most important people in my life who have supported and encouraged me unconditionally throughout my journey. I would like to express my profound gratitude to my dear parents for their immeasurable love and strong support. The unconditional care and belief in my abilities have been the driving force behind my success. From the very beginning, my parents have instilled in me the values of hard work, determination, and perseverance, shaping me into the person I am today. I am forever indebted to my parents for their faith in my dreams and for instilling the values of hard work, determination, and perseverance.

I am eternally grateful to my beloved wife, Priyanka, for her untiring love, understanding, and constant encouragement. My wife's presence by my side, through all the ups and downs, has made this journey not only bearable but also incredibly fulfilling. I would like to express my heartfelt appreciation to my brother, Chirag, and her wife, Anuja for their constant support, insightful perspective, and faith in my abilities have been invaluable. I would like to express my heartfelt gratitude to my father-in-law, Mr. Rajiv, and mother-in-law, Ms. Sunita, for their constant belief in me and unwavering support. Their presence in my life has been a source of strength and inspiration.

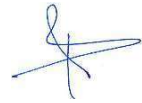
I would like to acknowledge the fellowship provided by the Ministry of Education, Govt of India, which helped me a lot financially. I am grateful to the Indian Institute of Technology (BHU) for the travel support to present my research at the conference (FENS Forum 2022) in Paris, France.

Moreover, I would like to express my sincere gratitude to eScience Institute-University of Washington, Seattle, USA for enriching my knowledge and skill by providing a great opportunity to attend their Neuroimaging and Data science training school. I was privileged to be 'Lead Teaching Assistant' for the international Computational Neuroscience course of the Neuromatch Academy USA and grateful to the organizer for giving me the opportunity. I am thankful to the National Centre for Biological Sciences, Tata Institute of fundamental research, Bengaluru, India, for hosting and supporting me during the training course.

Once again, I express my deepest gratitude to those who played an invaluable role in my academic pursuit.

Date: 27th July 2023

Place: Varanasi



(Pratik Purohit)

Dedicated to My Beloved Family

TABLE OF CONTENTS

LIST OF FIGURES	v
LIST OF TABLES	xiii
LIST OF ABBREVIATIONS AND SYMBOLS	xv
PREFACE	xvii
CHAPTER 1	1
Introduction	1
1.1 Perception of the Visual World:	1
1.2 Different factors affecting Visual Perception	6
1.2.1 External Factors	6
1.2.2 Internal Factors	13
1.3 Objectives of the Current Investigations:	23
CHAPTER 2	27
Alterations in Visual-Spatial Perception due to change in Autonomic Nervous System Activation	27
2.1 Introduction:	27
2.2 Formulation of the Quantitative Framework	31
2.2.1 The Geometry of Perceived visual space	31
2.2.2 Parameter for Representing the Alterations:	36
2.2.3 Dynamics of the Neuromodulating Agents in the Brain	40
2.2.4 Neural Correlates	43
2.2.4.1 Multi-Modal Sensory Perception System	43
2.2.4.2 Mapping of Visual Space by Grid Cells based Motif	45
2.2.4.3 Neuro-computational Model of Drug-Induced Perceptual Alterations ..	48
2.3 Experimental Validation of Quantitative Framework	54
2.3.1 Methodology	54
2.3.1.1 Dynamics of Psilocybin	54

2.3.1.2 Dynamics of Chlorpromazine	55
2.3.1.3 Diffusion MRI Experiment	56
2.3.1.4 Computational Model of a Grid Cell Network.....	57
2.3.1.5 Measurement of Visual Space Under Hyper-Activation.....	59
2.3.1.6 Spatial Distortion Threshold Under Hyper-Activation.....	61
2.3.1.7 Spatial Perception Under Hypo-Activation.....	62
2.3.2 Results.....	62
2.3.2.1 Visual Space under the Psilocybin-Induced Hyper-Activation	62
2.3.2.2 Relation between Drug Concentration and Perceptual Alterations.....	66
2.3.2.3 Prediction of Metric Tensor under Psilocybin-Induced Hyper-Activation.....	70
2.3.2.4 Visual Space under Chlorpromazine-Induced Hypo-Activation	72
2.3.2.5 Anatomical Connectivity between the Entorhinal Cortex and Area V2	75
2.3.2.5.1 Three Tesla MRI.....	75
2.3.2.5.2 Seven Tesla MRI	78
2.3.2.6 Grid Cell Activity under Drug-Induced Perceptual Alterations.....	79
2.3.2.6.1 During Normal Conditions (No Drug Condition)	79
2.3.2.6.2 Under Drug-Induced Neural Activation.....	80
2.3.2.6.3 Quantification of the drug-induced neural activation	85
2.4 Discussion	88
2.4.1 Quantitative Model	88
2.4.2 Verification by Empirical Finding	89
2.4.3 Practical Perspective:	90
2.4.4 Neuron-Level Processes:	91
2.4.5 Spectrum of Perceptual Modulation:.....	92
2.4.6 Biomedical Implications:.....	93
CHAPTER 3	95
Visual Perception of the Moving Object.....	95

3.1 Introduction	95
3.2. Our Mathematical Analysis	98
3.2.1 Geometrical Representation of Moving Object	98
3.2.2 Mapping Coordinate Transformations Between Retinotopic Space and Perceptual Space	100
3.2.3 Coordinate Transformation Matrix:	102
3.2.4 Generalization of Coordinate Transformation Matrix:	104
3.2.5 Relationship between Spatial Coordinates in Perceptual Space and Retinotopic Space	105
3.2.6 Translation to the Neural System.	109
3.3. Empirical Validation of the Mathematical Analysis	112
3.3.1 Methods	112
3.3.1.1 Moving Arc	112
3.3.1.2 Temporal Perception	113
3.3.2 Results	114
3.3.2.1 Perception of a Moving Arc	114
3.3.2.2 Perception of Time	118
3.4 Anatomical Correlates	121
3.4.1 Conceptual Observations	121
3.4.2 Diffusion MRI Tractography Experiment	123
3.4.2.1 Methods	123
3.4.2.2 Results	125
3.5. Proposed Neuronal Level Mechanism	136
3.6 Formal Analysis of the Perception of Moving Object	141
3.7 Discussions	146
3.7.1 Mathematical Model	146
3.7.2 Anatomical Correlates	147
3.7.3 Neuronal Framework	148
3.7.4 General Significance and Applicability	150

Chapter 4	151
Conclusion and Future Scope	151
4.1 Internal Factor	153
4.2 External Factor	157
4.3 Future Prospects	160
References	165
Appendix-A	205
List of Publications during Ph.D. Program	237

LIST OF FIGURES

Figure No.	Figure description	Page No.
Figure 1.1	Limited detection ranges of the human ear and human eye.	02
Figure 1.2	The brief outline of the process of visual perception.	02
Figure 1.3	The visual illusions show that perception and reality may not be the same. (a) The length of the two equal-length lines is perceived as unequal due to the presence of fins in the well-known Müller-Lyer illusion. (b) Two parallel lines are perceived as curved in the popular Hering illusion.	04
Figure 2.1	Conceptual illustration of the metric tensor for prototypical representative flat two-dimensional space and curved two-dimensional surface.	33
Figure 2.2	Conceptual illustration of the physical space and perceived visual space under the influence of the drug-induced activation of the autonomic nervous system.	33
Figure 2.3	Variation in modulation index (M) as drug concentration (C) changes, with different values of the n (Hill coefficient) and k (Half-effective drug concentration) for illustrative purposes.	39
Figure 2.4	Simplified two-dimensional cross-sectional representation of the brain as a porous medium.	40
Figure 2.5	Conceptual interconnection complex between the Entorhinal-Hippocampal network and the various local spatial maps at different sensory cortices (e.g., visual, auditory, olfactory, or somatosensory cortices), each sensory cortex is responsible for the metric-oriented representation of the perceived sensory space in that cortex.	46
Figure 2.6	a) Grid cells encode the navigational space by integrating the self-motion information for path integration. (b) Our formulation of the	47

metric representation of the visual space by grid cells by integrating the information about the eye movements for path integration like process.

- Figure 2.7** The arrangement of the nodes in the neural network model of the grid cells. 58
- Figure 2.8** Experimental setup to measure the geometry of the perceived vertical frontoparallel plane: Vertical central reference rod was placed one meter away from the subject. To avoid visual cues, the subject can see only mid-sections of the vertical peripheral rods and reference rod. The subject was instructed to move the peripheral vertical rods (towards or away from him) so that he/she could perceive all the rods in the same fronto-parallel plane. 59
- Figure 2.9** Experimental setup to measure the spatial distortion threshold using rotating prism lens: Rotating prism lens introduces the spatial distortion of the thick black horizontal line. The subjects view this black line through two prism lenses. The power of the second lens is kept fixed, while the power of the first lens is increased until the subject can perceive a just noticeable bending distortion in the black line. The spatial distortion threshold is measured by the minimum optical power of the first lens that is required for the subject to perceive the bending distortion. 61
- Figure 2.10** (a) Rotated ellipse represents the geometry of the perceived space under psilocybin administration. (b) The spherical coordinate system for locating a point in three-dimensional visual space. (c) Left panel: Alteration of Gaussian curvature of the perceptual space, the curvature being estimated at the fixation point O. Right panel: Alteration of the rotation angle of the perceptual space, the rotation being estimated from the perspective of the subject at the center of the ellipse. For both panels, the change in the alteration is shown at different time points after psilocybin ingestion. 63

- Figure 2.11** *Lower left panel:* The ellipse represents the geometry of the perceived space in the horizontal plane where ‘a’ and ‘b’ are the length of the major axis and minor axis (the ellipse is in the horizontal plane). Here, the subject is sitting at the center of the ellipse and looking along the y-axis, i.e., looking directly forward, while sitting in the experimental chair with a chin-rest. Before the experiment starts, the vertical rods are arranged in the vertical fronto-parallel plane. *Lower right panel:* The coordinate system for measuring the angular coordinate of a point on the ellipse. *Upper right panel (Inset box):* The alteration of the metric tensor at point O (fixation point), at four successive time points: time $t = 0$ (just before the experiment, no psilocybin given), then at time points $t = 90, 180,$ and 270 minutes after psilocybin ingestion. 65
- Figure 2.12** Psilocybin concentration in the brain’s extracellular space after oral ingestion. 66
- Figure 2.13** (a) Variation of the sum of squared residual with the Hill coefficient (n) and the Half-effect drug concentration (k). At $n = 14.8$ units (left panel) and $k = 1.39$ picomoles/cm³ (right panel), the sum of squared residual is minimum, showing the optimum fit. (b) The curve shows the mathematically calculated alterations in the metric tensor component of the perceptual space (solid line) while the Psilocybin concentration changes. The filled circles show the experimentally derived metric tensor components along with the corresponding value of the modulation index (M) and the time duration since the start of psilocybin ingestion (in minutes). Note the close correspondence of the experimental data-points to the theoretical curve. Indeed, the mathematical model is well validated by the experimentally-measured observations, which is further corroborated by robust satisfaction of the goodness-of-fit criterion (χ^2 statistical test firmly satisfied, $p > 0.99$). 68

Figure 2.14 (a) Metric tensor of the perceived space obtained from corresponding experimentally-measured spatial distortion threshold at four successive time points: time $t = 0$ (just before experiment, no psilocybin given), then at time points $t = 90, 180,$ and 270 minutes after psilocybin ingestion. (b) The metric tensor of perceptual space under the psilocybin induced hyperactivation condition. The theoretically computationally predicted values are shown in blue filled circle, while the experimentally-derived values are shown by the red cross. Observe the strong congruence of the experimental points with the theoretical points. Actually, the theoretical model is soundly validated by the empirical data as substantiated by strong satisfaction of goodness-of-fit criterion (there is robust satisfaction of the χ^2 -squared statistical test). 70

Figure 2.15 (a): Numerical values of the metric tensor components of the perceived space obtained from experimentally-recorded spatial distortion threshold at time $t=0, 210,$ and 450 minutes after ingestion of 50 mg oral intake of chlorpromazine. (b): Predicted chlorpromazine concentration (picomoles/cm³) in the brain's extracellular fluid as calculated from the theoretical computational model (chlorpromazine input is 50 mg). (c): The curve shows the predicted alteration in the theoretically computationally formulated metric tensor component of the perceptual space (solid line) while the Chlorpromazine concentration changes. The filled circles show the experimentally derived data-points estimating the metric tensor components. For each experimental data-point, there is shown the time duration since the start of chlorpromazine ingestion (in minutes). Note the close correspondence of the experimental data-points to the theoretical computational curve. Indeed the 73

mathematical model is well corroborated by the experimentally-measured observations.

- Figure 2.16** Anatomical connectivity (neural tracts) between the entorhinal cortex and visual cortex (area V2) in the sixteen subjects obtained after performing the tractography experiment. 75
- Figure 2.17** Anatomical connectivity (neural tracts) between the entorhinal cortex and visual cortex (area V2), obtained from MRI-tractography analysis of the fourteen subjects (Subject 17 to 30). 76
- Figure 2.18** Anatomical connectivity (neural tracts) between the entorhinal cortex and visual cortex (area V2), obtained from MRI-tractography analysis of the 7 Tesla diffusion MRI scan. (Cognitively normal, female, 27 years) 78
- Figure 2.19** Activity of the neuronal nodes under no-drug condition (a) when eyes are not moving and fixating in the visual field (b) when eyes are making a constant movement in the visual field (c) when eyes are randomly scanning in the visual field. (d) Variation in the angular position of the eyeball movements during constant eye movement (upper) and random eye movement (lower). 80
- Figure 2.20** Activity of the neuronal nodes under drug-induced activation (eye fixation): (a) Activation pattern of the nodes under the different values of the $\Delta I=0.05, 0.15, 0.25,$ and 0.30 . (b) Variation in the activity of node number 47 as the ΔI changes from 0 to 0.30 . 82
- Figure 2.21** (a) Change in the periodic activation of the neuronal nodes for different values of the ΔI . (b) Activity of the neuronal node 47 for the different values of the ΔI and time. (c) Variation in the angular coordinates of the moving fixation point. At the origin, $t=0$ second: $\theta=0$ and $\Phi=0$; thereafter, θ and Φ are increasing linearly with time, indicating that eyes move with a constant velocity across both angular directions. 83

Figure 2.22	(a) Activity pattern of the neuronal nodes for the different values of the ΔI , as the eyeball is moving randomly in the visual field. (b) Temporal variation in the activity of neuronal node 47 for the different values of ΔI . (c) Variation in the angular coordinates of the randomly moving fixation point.	84
Figure 2.23	(a) Spatiotemporal distance (L) for a particular value of the ΔI . We calculated L for the different values of the ΔI . (b) Experimentally calculated activity index (filled circles) using the neural network-based model of grid cell network model, and the corresponding Hill equation curve is also shown. (c) & (d) Variation of the sum of squared residual with the Hill coefficient (n) and k . At $n=1.8$ and $k=0.07$, the sum of squared residuals is minimum and optimally fits the observed data points.	85
Figure 3.1	Changes in spatial position of the moving object with time in the retinotopic map.	98
Figure 3.2	Transformation of the representation of the moving object from retinotopic space to perceptual space.	99
Figure 3.3	The cortical magnification factor denotes the cortical tissue involved in the retinotopic representation of the given size of the visual field. The cortical magnification factor is the ratio of the size of the cortical tissue (z) and the visual angle subtended on the eye (θ).	110
Figure 3.4	Our formulation of perception of a moving object: The moving object is projected on the retinotopic map through the retinal surface and follows the cortical magnification factor for mapping from the visual field to the retinotopic map. Then, transformation equations relate the spatiotemporal coordinate of the moving object in the retinotopic and perceptual space. After that, on applying the inverse cortical magnification factor provides the coordinates of the perceived moving object at the scale of physical space.	111

Figure 3.5	Experimental setup for measuring the perceived length of a moving arc at different speeds.	113
Figure 3.6	Alteration in the perceived length of the moving arc at different rotational speeds of the arc.	115
Figure 3.7	Constancy of the fidelity parameter k , while rotational speed of moving arc changes. This constancy validates the theoretical prediction of our mathematical model. (Statistical goodness-of-fit test satisfied, $p > 0.99$).	117
Figure 3.8	Experimental observations of the reproduction method (second experiment) validates the theoretical prediction of our mathematical model. (Statistical goodness-of-fit test satisfied, $p > 0.99$).	120
Figure 3.9	Experimental observations of the matching method (first experiment) validates the theoretical prediction of our mathematical model. (Statistical goodness-of-fit test satisfied, $p > 0.99$).	120
Figure 3.10	Pathways for spatio-temporal interaction (Subject A, MRI 3 tesla scanner). Upper Row: Tracts between middle temporal visual area (V5) and brain regions active during time perception. Middle Row: Tracts between middle temporal visual area (V5) and brain regions active during spatially locating of an object. Lower Row: Tracts between left and right middle temporal visual area (V5). (The brain regions are listed in Table 3.1).	129
Figure 3.11	Pathways for spatiotemporal interaction (Subject B, MRI 7 tesla scanner): Upper Row: Tracts between middle temporal visual area (V5) and brain regions active during time perception. Middle Row: Tracts between middle temporal visual area (V5) and brain regions active during spatially locating an object. Lower Row: Tracts	130

between left and right middle temporal visual area (V5). (The brain regions are listed in Table 3.1).

- Figure 3.12** Time Perception: Neural tracts between middle temporal visual area (V5) and brain regions active during time perception for the Subject 1 to Subject 14. 132
- Figure 3.13** Time Perception: Neural tracts between middle temporal visual area (V5) and brain regions active during time perception for the Subject 15 to Subject 30. 133
- Figure 3.14** Spatial location perception: Neural tracts between middle temporal visual area (V5) and brain regions active during spatially locating an object for the subject 1 to subject 16. 134
- Figure 3.15** Spatial location perception: Neural tracts between middle temporal visual area (V5) and brain regions active during spatially locating an object for the subject 17 to subject 30. 135
- Figure 3.16** Temporal dynamics of acetylcholine concentration and dopamine concentration. 139
- Figure 3.17** (a) Alteration of the phase shift between the oscillatory concentrations of dopamine (or Acetylcholine), while the acetylcholine-dopamine interaction parameter varies. (b) Alteration of the oscillation time period of Acetylcholine (or dopamine), while the acetylcholine-dopamine interaction parameter varies. 139
- Figure 3.18** Biochemical basis of the interaction of the spatial information stream and the temporal information stream during the perception of a moving object, the interaction occurring at the axodendritic synapse. 141
- Figure 3.19** (a) Vectorial representation of the interaction between the Spatial information stream (X) and the Time information stream (T). (b) Interaction between the orthogonal components of the time information stream and spatial information stream 142

LIST OF TABLES

Table No.	Table description	Page No.
Table 2.1	Different parameters related to the neural tracts obtained between the entorhinal cortex and area V2.	77
Table 3.1	Brain regions active during perception of time and perception of spatial location of an object.	125
Table 3.2	Eigenvector centrality and PageRank centrality of the different brain regions as nodes of the network for Subject-A regarding time perception and spatial perception.	127
Table 3.3	Eigenvector centrality and PageRank centrality of the different brain regions as nodes of the network for Subject B regarding time perception and spatial perception.	128
Table 3.4	Fiber tract parameters related to the neural tracts connecting the area V5 and brain regions active during time perception for subjects 1 to 30.	136
Table 3.5	Fiber tract parameters related to the neural tracts connecting the area V5 and brain regions active during locating an object for subjects 1 to 30.	136

LIST OF ABBREVIATIONS AND SYMBOLS

LSD	Lysergic acid diethylamide
MRI	Magnetic Resonance Imaging
M	Modulation Index
n	Hill Coefficient
TS	Tortuosity
α	Volume fraction
k_{pi}	Transfer coefficient for the drug molecules from the blood to the brain tissue
k_{po}	Transfer coefficient for the drug molecules from brain tissue to the blood
C	Drug concentration in the extracellular space
C_a	Drug concentration in plasma
3D	Three dimensional
N	Total number of nodes
λ	Stabilization strength
W_{ij}	Connection weight between node P_i and P_j
T	Ratio of the excitatory and inhibitory connections
I	Interaction strength
GABA	Gamma-aminobutyric acid
ECS	Extra Cellular Space
D	Diffusivity
OASIS	Open Access Series of Imaging Studies
AC-PC	Anterior Commissure - Posterior Commissure
DWI	Diffusion Weighted Imaging
EPI	Echo Planar Imaging
TR	Repetition Time
TE	Time to Echo
FSL	FMRIB Software Library
β	Minimum prism power

AI	Activation Index
EEG	Electroencephalography
V1	Primary Visual Cortex
fMRI	Functional Magnetic Resonance Imaging
Z	Transformation matrix
P	Speed of moving object in the retinotopic space
γ	Cortical magnification factor
χ^2	chi-square
MT/V5	Middle temporal visual area
HARDI	High Angular Resolution Diffusion Imaging
3T	Three Tesla
7T	Seven Tesla
m	Interaction parameter

PREFACE

Visual perception is the process by which our brains interpret and make sense of the information received through eyes. Visual perception is a fundamental aspect of human experience, allowing us to perceive, recognize, and understand the world. The process begins with the capture of light by the eye's retina, where specialized cells, namely photoreceptors, convert the light into electrical signals. Electrical signals are then transmitted to the brain via the optic nerve, where they are further processed and interpreted to create a visual experience. Visual perception gives the ability to perceive colors, shapes, sizes, depth, and motion, enabling us to navigate the complex environment, recognize objects, and interact meaningfully with the world.

Visual perception is a complex and subjective experience. Sensory illusions provide compelling evidence that visual perception is not a fixed representation of objective reality, but exhibits variations and inconsistencies. Due to sensory illusions, perception diverges from the physical properties of a stimulus, showcasing the influence on visual perception. Sensory illusions underscore the dynamic nature of perception by modifying the relationship between the physical world and the perceived world. To underscore, visual perception can be shaped by a multitude of factors.

Various external factors, including the presence of other stimuli, lighting conditions, motion, and contextual cues, influence visual perception. These external factors of the surrounding modify and shape the perception of visual information, affecting contrast detection, brightness perception, object recognition, perceived size, and depth evaluation. Similarly, visual perception is also influenced by a range of internal factors of the personal subject, including sensory adaptation, expectations and beliefs, emotions, cognitive biases,

individual differences, and the effects of biochemical or neuro-pharmaceutical agents. The effects of such biochemical agents on visual perception can be diverse, with neuroactive substances causing distortions and heightened sensitivity, stimulant agents intensifying visual acuity, and depressant agents impairing perception. For instance, ketamine (or pharmaceutical) can lead to variable effects on visual perception depending on the individual susceptibility, dose concentration, and bioavailability. These internal factors play a significant role in shaping visual perception and highlight the complex nature of human cognition.

A quantitative understanding of the effect of modulatory factors can provide valuable insights into the mechanisms of perception and have implications in psychology, neuroscience, cognitive technology, neuropsychiatry, and human-computer interaction. In our thesis, we focused on two factors: how visual perception is affected by the activation of the sympathetic or parasympathetic nervous system (internal factor) and by the object's movement (external factor) affect visual perception.

In the chapter 1 of the thesis, we have provided a broad introduction and prospects of the research problem and provide a delineation of the approach that we take.

Thereafter in chapter 2, we presented a quantitative framework to formulate the variations in visual-spatial perception due to the sympathetic or parasympathetic nervous system activation. By considering the dose amount of the biochemical agent or drug which can induce autonomic nervous system activation, we quantified the activation levels. Using the metric tensor to quantify visual space, we established a relationship between (i) the concentration of the neuromodulator/drug concentration and (ii) the visual-spatial alterations, by utilizing the Hill equation of the chemical reaction kinetics. We then analyzed independent experimental studies using our model and found a close validation ($p > 0.99$) between our

theoretical mathematical predictions and the observed experimental findings, characterized by the values of Hill coefficient (n) = 14.8 and k = 1.39 for psilocybin. We successfully predicted and verified the outcome of another experiment with psilocybin using the same values of the system parameters (n = 14.8 and k = 1.39). Additionally, we found that visual-spatial perception modulation closely matched our model under hypoactivation state induced by chlorpromazine, a relaxant pharmaceutical (χ^2 ; $p > 0.99$).

To explain the aforesaid altered visual-spatial perception, we computationally formulated a grid cell-based theoretical framework. Validating our framework, we simulated the effect of a neuromodulating pharmaceutical agent on the computational model of the grid-cell network and observed activity changes that verified the functionality of our model. Furthermore, diffusion MRI-based tractography on human brain scans were performed which revealed the neural tracts connecting the nodal cortical areas for visual-spatial perception in our framework: V2 and the entorhinal cortex. Our quantitative approach holds considerable potential for behavioral screening and for treatment-monitoring tools in neuropsychological cognitive disorders.

Next, we focused on the external factor (motion) in Chapter 3. Our quantitative model established a mathematical relationship between the spatiotemporal coordinates of the external object and of the perceived object; this we undertook by transforming the perception of the moving object from retinotopic space to perceptual space. Through coupled linear equations, our model demonstrated the interaction between visual-spatial and temporal perception. Analyzing the constancy of temporal causality, our model showed that the speed of a moving object influences both visual-spatial and temporal perception. Validated through two experiments, our model accurately predicted their behavioral findings (χ^2 ; $p > 0.99$).

Furthermore, we performed another MRI tractography experiment which showed that the cerebral area V5 may be the anatomical site for the interaction between visual-spatial and temporal perception. Additionally, we formulated a Lotka-Volterra system-type model to analyze the interplay between acetylcholine and dopamine neurotransmitters, exhibiting periodic oscillations. These oscillations may modulate visual perception by influencing the tuning properties of complex cells in cerebral area V5. Our study represented an innovative significant, and validated endeavor to connect motion perception with causality invariance mathematically.

In Chapter 4, we presented the main conclusions and outlined potential future prospects for our studies.